Choi for suggesting this problem. Thanks are also due to Professor Choi, Professor John Hernandes, Professor K. S. Dy, and Dr. N. D. Lang for reading the manuscript and making helpful comments.

[1]E. Wigner and J. Bardeen, Phys. Rev. 48, 84 (1935); J. Bardeen, ibid. 49, 653 (1936).

[2]H. B. Huntington, Phys. Rev. 81, 1035 (1951).

[3]N. D. Lang and W. Kohn, Phys. Rev. B 1, 4555 (1970); N. D. Lang, Solid State Commun. 7, 1047 (1969); N. D. Lang and W. Kohn, Phys. Rev. B 3, 1215 (1971).

Theory of Radiative Heat Transfer between Closely Spaced Bodies

D. Polder and M. Van Hove

Philips Research Laboratories, N. V. Philips' Gloeilampenfabrieken, Eindhoven, Netherlands

(Received 28 January 1971)

A general formalism is developed by means of which the radiative heat transfer between macroscopic bodies of arbitrary dispersive and absorptive dielectric properties can be evaluated. The general formalism is applied to the heat transfer across a vacuum gap between two identical semi-infinite bodies at different temperatures. The peculiarities arising when the gap width is of the order of, or smaller than, the dominant thermal radiation wavelengths are studied and quantitatively evaluated for the case of two metal bodies. The predicted strong increase with diminishing gap width is in qualitative agreement with experimental results.

I. INTRODUCTION

Consider a set of bodies of macroscopic dimensions with arbitrary dispersive and absorptive dielectric properties. These bodies emit thermal radiation depending on the local temperature. With the aid of the fluctuation-dissipation theorem and electromagnetic theory we shall derive a formula for the heat flux at an arbitrary point due to the radiating bodies. Integration of this heat flux over a closed surface gives the net power dissipated in the absorbing matter contained in the enclosed volume.

By this method we intend to determine and discuss the net heat transfer between two semi-infinite absorbing bodies with arbitrary dielectric properties at slightly different temperatures separated by vacuum of width d. The heat transfer between closely spaced bodies differs from that when the spacing is large for two reasons. Firstly, when the separation d is comparable to, or smaller than, the dominant vacuum wavelengths at the temperatures considered, interference effects must be expected in the waves multiply reflected between the two surfaces. Secondly, the evanescent fields normally present in thermal equilibrium at the outer surface of each body can reach over to the opposite body and transfer energy if the distance is sufficiently small. As will be explicitly shown for metal bodies, the latter mechanism of energy transfer is the dominant one for small distances, giving rise to a strong increase of heat transfer with decreasing d.

Rytov has developed a treatment of problems of this kind. Rytov's work and ours differ in the following respects. One difference is merely formal: Rytov starts from random thermal exciting electromagnetic fields, for which he writes down a correlation function, in which a constant factor C appears. In Ref. 1, C is determined *a posteriori* by reproducing Kirchhoff's law for radiation emitted into vacuum. In Ref. 2, C is obtained from Nyquist's formula, and a discussion of the zero correlation radius used by him (and by us) appears. In our work we take electric currents rather than fields as the random thermal sources and use the fluctuation-dissipation theorem to determine their statistical properties; this rather simplifies the formal treatment.

The second difference is that Rytov's study of the heat transfer across a gap is confined to the case of one semi-infinite absorbing body at temperature T separated by vacuum from an almost perfect mirror at zero temperature: The mirror is described by the approximate boundary conditions of Leontovich, which state that the magnetic fields are the same as if the mirror were perfect. In our work we study the heat transfer between two arbitrary identical semi-infinite bodies at different temperatures, while exact boundary con-

ditions are used. In addition we present a thorough and quantitative analysis of the distance and temperature dependence of the heat transfer between metal bodies. A comparison of our formulas and Rytov's for the case of highly reflecting metals shows similarity in over-all features but reveals discrepancies in detail, which we ascribe to the use of approximate boundary conditions by Rytov.

A related problem has been considered by Cravalho et al.[3] and Olivei,[4] viz., the heat transfer across a vacuum gap between two semi-infinite nondispersive nonabsorptive media, in which the origin of the thermal radiation is unspecified.

The problem of the heat transfer between closely spaced bodies was taken up independently by Hargreaves, who has also shown the existence of proximity effects experimentally.[5] It was his interest that prompted us to carefully reinvestigate the theoretical aspects of the problem and in particular to concentrate our attention to transfer between metals. In Hargreaves's experiments chromium layers were used as emitting bodies, and for this reason a numerical analysis of the case of chromium is included as an example in our paper.

In Sec. II of this paper we shall present a theory that is generally valid within the following limits: (i) continuum electromagnetic treatment (macroscopic Maxwell's equations); (ii) zero correlation radius for electric currents; (iii) isotropic nonmagnetic substances; (iv) stationary in time with local thermodynamic equilibrium. There we also specialize to problems with translational symmetry in two directions. Section III solves Maxwell's equations for layered media. In Sec. IV the theory will be applied in some detail to the case of radiation of a semi-infinite body into vacuum (yielding Kirchhoff's law). In Sec. V the problem of radiative heat transfer between two semi-infinite bodies will be solved. In Sec. VI the general result of Sec. V will be reformulated so that generalized transmission coefficients t appear in the expression. The structure of the t's and their influence on the integrated result will be discussed with special reference to materials of high reflectivity. In Sec. VII an attempt will be made to extract the dependence of the result on the various parameters (gap width, temperature, material constants) in the case of strongly absorbing metals. Numerical integration will be used to illustrate the case of a realistic material, for comparison with experiment.

It is worth pointing out that the final expression for the heat transfer depends in such a complex way on the specific dielectric properties of the material, that it does not seem possible to foresee immediately even qualitatively the behavior of the result for an arbitrary material.

II. METHOD

The technique used starts from a macroscopic description of the substance considered, together with a postulated form of the fluctuation-dissipation theorem applying to the thermally fluctuating microcurrents in the substance which constitute the sources of the thermal radiation emitted by the substance. We have

$$\mathrm{curl}\,\vec{H} = \frac{1}{c}\frac{\partial \vec{E}}{\partial t} + \frac{4\pi}{c}\vec{j}_{\mathrm{ind}} + \frac{4\pi}{c}\vec{j}_{\mathrm{source}} \ ,$$

$$\mathrm{curl}\,\vec{E} = -\frac{1}{c}\frac{\partial \vec{H}}{\partial t} \ . \tag{1}$$

Here the inhomogeneous term $\vec{j}_{\mathrm{source}}(\vec{x}, t)$ is the thermal random current density source, while $\vec{j}_{\mathrm{ind}}(\vec{x}, t)$ comprises all induced current densities in the substance due to the presence of the electromagnetic field. We assume that the substance is nonmagnetic and isotropic and that a local relation holds between $\vec{j}_{\mathrm{ind}}(\vec{x}, t)$ and $\vec{E}(\vec{x}, t)$ in such a way that we may write for each frequency component

$$\frac{1}{c}\frac{\partial \vec{E}}{\partial t} + \frac{4\pi}{c}\vec{j}_{\mathrm{ind}} = \frac{i\omega}{c}\epsilon(\omega)\vec{E} \ .$$

The dielectric constant $\epsilon(\omega) = \epsilon' - i\epsilon''$ is complex and contains in its imaginary part all the dissipative properties of the substance.

The ω component of any quantity $G(t)$ is defined as

$$G(\omega) = (2\pi)^{-1/2}\int_{-\infty}^{+\infty} dt\, e^{-i\omega t} G(t) \ , \tag{2}$$

and will be used for $\omega > 0$ only.

Thus, we have

$$\mathrm{curl}\,\vec{H}(\vec{x}, \omega) = \frac{i\omega}{c}\epsilon(\vec{x}, \omega)\vec{E}(\vec{x}, \omega) + \frac{4\pi}{c}\vec{j}_{\mathrm{source}}(\vec{x}, \omega) \ ,$$

$$\mathrm{curl}\,\vec{E}(\vec{x}, \omega) = -\frac{i\omega}{c}\vec{H}(\vec{x}, \omega) \ . \tag{3}$$

The ω component $\vec{j}(\vec{x}, \omega)$ of the source $\vec{j}(\vec{x}, t)$ is a (Gaussian) random variable which, according to the fluctuation-dissipation theorem, obeys the relation

$$\langle j_a(\vec{x}, \omega) j_b^*(\vec{x}', \omega') \rangle = (2\pi)^{-1}\epsilon''(\vec{x}, \omega)\hbar\omega^2$$

$$\times (e^{\hbar\omega/kT} - 1)^{-1}\delta(\omega - \omega')\delta(\vec{x} - \vec{x}')\delta_{ab} \ , \tag{4}$$

while $\langle j, j \rangle = \langle j^*, j^* \rangle = 0$; $\hbar$ and kT have their usual meaning and $\langle \rangle$ is the ensemble average. The spatial independence of current sources at different points is compatible with the assumed local properties of the medium, the independence of the different vector components $(a, b = x, y, z)$ with the assumed isotropy.

It is difficult to give more than a qualitative discussion of the limit of validity of the phenomeno-

logical approach described here, since it will much depend on the physics of the material involved. For instance, if we have a metal whose "optical" properties are largely determined by the conduction electrons and these electrons have a long mean free path, then we expect that any contributions from spatial Fourier components shorter than that mean free path will be inadequately dealt with in the present treatment. Related to this is a limitation on minimum geometric dimensions such as radii of curvature or thicknesses or distances. Also, materials for which the optical properties are affected by phenomena such as the anomalous skin effect are excluded from the present treatment.

For the purpose of calculating the radiative energy transfer we shall need the ensemble average of the Poynting vector

$$\vec{S}(\vec{x}, t) = (c/4\pi)\vec{E}(\vec{x}, t) \times \vec{H}(\vec{x}, t)$$

at suitable points $\vec{x}$. Because of Maxwell's equations, each field in this expression is itself proportional to current sources at all points $\vec{x}'$ of the emitting body. For instance we have, $\overleftrightarrow{e}$ being a tensor,

$$\vec{E}(\vec{x}, t) = (2\pi)^{-1/2} \int_0^\infty d\omega' \int d\vec{x}' e^{i\omega' t}$$

$$\times \overleftrightarrow{e}(\vec{x}, \vec{x}', \omega')\vec{j}_{\text{source}}(\vec{x}', \omega') + \text{c.c.} \quad , \quad (5)$$

and a similar expression for $\vec{H}(\vec{x}, t)$. The expression for $\langle \vec{S}(\vec{x}, t) \rangle$ is then an eightfold integral over ω', ω'', $\vec{x}'$, $\vec{x}''$ involving $\langle j_a(\vec{x}', \omega')j_b^*(\vec{x}'', \omega'')\rangle$. Because of Eq. (4) this reduces to a fourfold integral over ω' and $\vec{x}'$, showing that each volume element, each frequency component, and each vector component of the source contribute independently.

The result then takes on the following form in obvious notation:

$$\langle \vec{S}(\vec{x})\rangle = \tfrac{1}{2}(2\pi)^{-3} c \sum_a \int d\omega\, d\vec{x}' \, \vec{e}_a(\vec{x}, \vec{x}', \omega)$$

$$\times \vec{h}_a^*(\vec{x}, \vec{x}', \omega)\hbar\omega^2(e^{\hbar\omega/kT(\vec{x}')} - 1)^{-1}\epsilon''(\vec{x}', \omega) + \text{c.c.}$$

Thus the heat flux in any point $\vec{x}$ is found as soon as the tensors $\overleftrightarrow{e}$ and $\overleftrightarrow{h}$ have been determined, which can be done by solving Maxwell's equations in the desired geometry with $\vec{j}_0 \delta(\vec{x} - \vec{x}')e^{i\omega t}$ as point sources.

If the problem shows translational symmetry in, say, the x and y directions, this is best taken advantage of by introducing the x and y Fourier components of the fields and the current sources. Thus, we have

$$\vec{E}(\vec{x}, t) = (2\pi)^{-3/2} \int_0^\infty d\omega' \int\int_{-\infty}^{+\infty} dk_x'\, dk_y'$$

$$\times e^{i(\omega' t - k_x' x - k_y' y)}\vec{E}(k_x', k_y', z, \omega') + \text{c.c.} \quad , \quad (6)$$

and, because of translational symmetry,

$$\vec{E}(k_x, k_y, z, \omega)$$

$$= \int dz' \overleftrightarrow{e}(k_x, k_y, z, z', \omega)\vec{j}_{\text{source}}(k_x, k_y, z', \omega) \quad (7)$$

defines the tensor $\overleftrightarrow{e}(k_x, k_y, z, z', \omega)$. Similar expressions hold for $\vec{H}^*(k_x, k_y, z, \omega)$. With the aid of Eq. (4) one easily deduces the ensemble average

$$\langle j_a(k_x, k_y, z, \omega) j_b^*(k_x', k_y', z', \omega')\rangle$$

$$= (2\pi)^{-1}\epsilon'' \hbar\omega^2(e^{\hbar\omega/kT} - 1)^{-1}\delta(\omega - \omega')$$

$$\times \delta(k_x - k_x')\delta(k_y - k_y')\delta(z - z')\delta_{ab} \quad , \quad (8)$$

so that finally we have

$$\langle \vec{S}(z)\rangle$$

$$= \tfrac{1}{2}(2\pi)^{-5} c \sum_a \int d\omega\, dk_x\, dk_y\, dz'\, \vec{e}_a(k_x, k_y, z, z', \omega)$$

$$\times \vec{h}_a^*(k_x, k_y, z, z', \omega)$$

$$\times \hbar\omega^2(e^{\hbar\omega/kT} - 1)^{-1}\epsilon'' + \text{c.c.} \quad , \quad (9)$$

where, of course, ϵ'' and T may still be functions of z'.

III. SOLVING MAXWELL'S EQUATIONS

We must determine the tensors $\overleftrightarrow{e}(k_x, k_y, z, z', \omega)$ and $\overleftrightarrow{h}(k_x, k_y, z, z', \omega)$. Therefore, we calculate the electromagnetic fields due to a current source of the form

$$\vec{j} = \vec{j}_0 \delta(z - z') e^{i(\omega t - k_x x - k_y y)} \quad . \quad (10)$$

Without loss of generality we can confine ourselves to the case $k_y = 0$, as the problem now has azimuthal symmetry.

The medium in which these sources are present will consist of layers perpendicular to the z axis, each layer having a constant ϵ. The space can then be divided into sections, in each of which the field will consist of a combination of two waves:

$$\vec{A} e^{i(\omega t - k_x x \pm k_z z)} \quad (\vec{A} = \vec{E} \text{ or } \vec{H}) \quad , \quad (11)$$

with $k_x^2 + k_z^2 = \epsilon\omega^2/c^2$ and in which $\text{Im}\,k_z \leqslant 0$, $\text{Re}\,k_z \geqslant 0$ ($\text{Im}\,\epsilon \leqslant 0$). The complex amplitude $\vec{A}$ shows jumps at the boundaries of the layers and at the plane $z = z'$ of the source. The jumps at the boundaries of the layers are determined by the usual conditions, E_x, E_y, H_x, H_y continuous across the boundaries, while for those sections extending to $\pm\infty$ only one wave with, respectively, $-k_z$ and $+k_z$ will be present. The jumps at $z = z'$ will be discussed now.

A source

$$j_x = j_{0x}\delta(z - z')e^{i(\omega t - k_x x)}$$

causes a jump in H_y equal to

$$\Delta H_y\big|_{z=z'} = -4\pi c^{-1} j_{0x} e^{i(\omega t - k_x x)} \quad , \quad (12)$$

while H_x, E_x, E_y are continuous.

A source

$$j_y = j_{0y}\, \delta(z - z')e^{i(\omega t - k_x x)}$$

causes a jump in H_x equal to

$$\Delta H_x \big|_{z=z'} = 4\pi c^{-1} j_{0y} e^{i(\omega t - k_x x)} \quad , \tag{13}$$

while H_y, E_x, E_y are continuous.

A source

$$j_z = j_{0z}\, \delta(z - z')e^{i(\omega t - k_x x)}$$

causes a dipolar layer with a potential jump equal to

$$- 4\pi i(\omega \epsilon)^{-1} j_{0z}\, e^{i(\omega t - k_x x)}$$

which in turn causes a jump in E_x given by

$$\Delta E_x \big|_{z=z'} = 4\pi k_x (\omega \epsilon)^{-1} j_{0z}\, e^{i(\omega t - k_x x)} \quad . \tag{14}$$

Now E_y, H_x, H_y are continuous.

All further discontinuities in the field quantities or their derivatives at $z = z'$ follow from those given above.

The combined boundary conditions at the boundaries of the layers, at the source, and at infinity suffice to determine the electromagnetic fields $E_a(k_x, 0, z, z', \omega)$ and $H_a(k_x, 0, z, z', \omega)$ due to the given source at z'. For example, according to Eq. (7) the tensor $\overleftrightarrow{e}$ for $k_y = 0$ then follows from

$$E_a(k_x, 0, z, z', \omega) = \sum_b e_{ab}(k_x, 0, z, z', \omega)j_{0b} \quad , \tag{15}$$

and similarly for $\overleftrightarrow{h}$.

We will complete the solution of Maxwell's equations in two specific cases.

IV. FIRST APPLICATION: RADIATION INTO VACUUM

If the half-space $z < 0$ is filled by a medium with dielectric constant $\epsilon(\omega)$ and temperature T, and for $z > 0$, $\epsilon = 1$ (vacuum), Kirchhoff's law states that the amount of energy radiated into a solid angle $d\Omega$ at an angle ϑ from the z axis and a frequency interval $d\omega$ is given by

$$I_\omega\, d\omega\, d\Omega$$

$$= (1 - R_{\parallel} + 1 - R_{\perp})(2\pi)^{-3}\hbar\omega^3 c^{-2}(e^{\hbar\omega/kT} - 1)^{-1}d\omega\, d\Omega \quad . \tag{16}$$

Here $R_{\parallel}$ and $R_{\perp}$ are the reflection coefficients for the two polarization states of a light beam incident at the angle ϑ. As is well known, Kirchhoff's law can be derived with the aid of a simple thermodynamic argument from the thermal equilibrium radiation density in vacuum.

The purpose of this section is to show how this result is obtained with the aid of the procedure outlined in the preceding sections. It will also serve to discuss a few points which will be of importance for the more complicated problem of the radiative transfer between two bodies to be dealt with in the

second application. We shall first calculate the electromagnetic fields at $z > 0$ as produced by a source $\vec{j}_0\, \delta(z - z')e^{i(\omega t - k_x x)}$ $(z' < 0)$. We shall distinguish between two states of polarization, the $\parallel$ polarization for which $E_y = H_x = H_z = 0$, and the $\perp$ polarization, for which $E_x = E_z = H_y = 0$. From the nature of the singularities at the source it is easily seen that the components j_x and j_z only excite $\parallel$ waves, while j_y only excites $\perp$ waves.

For waves of either type of polarization, we have one wave decaying towards $z \to -\infty$ in the region $z < z'$, two waves in the region $z' < z < 0$, one decaying to the right and one to the left, and in the vacuum region one wave propagating or decaying towards $z \to \infty$. These four fields can be expressed in terms of $\vec{j}_0$ with the aid of four boundary conditions, two for the field components parallel to the surface at $z = 0$ and two for the plane $z = z'$.

For the $\parallel$ polarization we find, for instance, for $z > 0$,

$$H_y = - 4\pi c^{-1}(\epsilon k_{zv} + k_z)^{-1}(k_z j_{0x} - k_x j_{0z})$$

$$\times e^{i(\omega t - k_x x - k_{zv} z + k_z z')};$$

while for the $\perp$ polarization we have, for instance,

$$E_y = - 4\pi \omega c^{-2}(k_{zv} + k_z)^{-1} j_{0y} e^{i(\omega t - k_x x - k_{zv} z + k_z z')} \quad ,$$

where $k_x^2 + k_z^2 = \epsilon \omega^2/c^2$ and $k_x^2 + k_{zv}^2 = \omega^2/c^2$. The full tensors $\overleftrightarrow{e}$ and $\overleftrightarrow{h}$ at $k_y = 0$ easily follow from these expressions.

As long as $|k_x| < \omega/c$, these fields represent plane waves (k_{zv} real) propagating at angle $\vartheta = \arctan(k_x/k_{zv})$. For $|k_x| > \omega/c$ these fields constitute evanescent waves with vanishing amplitude as $z \to \infty$. The latter waves do not contribute to the emitted radiation. As is well known the average energy flow in these waves is parallel to the surface.

The total radiation into a solid angle $d\Omega = c^2\omega^{-2}(\cos\vartheta)^{-1}dk_x\, dk_y$ within the frequency interval $d\omega$ is therefore obtained by integrating the integrand of Eq. (9) only over z' from $-\infty$ to 0. This integration gives a factor

$$\int_{-\infty}^{0} dz'\, \exp(i(k_z - k_z^*)z') = -\tfrac{1}{2}(\mathrm{Im}\, k_z)^{-1} \quad ,$$

and we have finally

$$I_\omega\, d\omega\, d\Omega$$

$$= 2(2\pi)^{-3}\hbar\omega^3 c^{-2}(e^{\hbar\omega/kT} - 1)^{-1}\epsilon''(-\mathrm{Im}\, k_z)^{-1}k_{zv}$$

$$\times \left(\frac{k_x^2 + k_z k_z^*}{|\epsilon k_{zv} + k_z|^2} + \frac{\omega^2}{c^2}\frac{1}{|k_{zv} + k_z|^2} \right) d\omega\, d\Omega \quad , \tag{17}$$

where the two terms between the large parentheses originate, respectively, from $\parallel$ and $\perp$ polarized waves.

The energy reflection coefficients of these two waves at the angle of incidence ϑ can be written as

$$R_{\parallel} = \left| \frac{\epsilon k_{zv} - k_z}{\epsilon k_{zv} + k_z} \right|^2 \;, \quad R_{\perp} = \left| \frac{k_{zv} - k_z}{k_{zv} + k_z} \right|^2 \;. \qquad (18)$$

With the aid of the relations

$$\text{Re}(\epsilon/k_z) = c^2 \omega^{-2}(k_x^2 + k_z k_z^*)\text{Re}(k_z)|k_z|^{-2}$$

and

$$\epsilon'' = -2c^2 \omega^{-2}\text{Re}k_z \,\text{Im}k_z \;,$$

and recalling that we deal with azimuthal symmetry about the z axis, one demonstrates the equivalence of Eq. (17) and the Kirchhoff formula, Eq. (16).

V. HEAT TRANSFER BETWEEN TWO BODIES

If the half-space $z < 0$ is filled by a medium with dielectric constant $\epsilon_1(\omega)$ and temperature T_1 and the half-space $z > d$ is filled by a medium with $\epsilon_2(\omega)$ and T_2, the region $0 < z < d$ being vacuum (cf. Fig. 1), the radiative transfer of heat can be calculated in the following way.

We first consider the fields set up by the noise sources in the medium at $z < 0$ and calculate the (averaged) Poynting vector in the z direction at the point d_+, i. e., just inside the second medium. This is the heat transferred to the second medium due to the thermal radiation from the first. In the same way we calculate the Poynting vector in the $-z$ direction at $z = 0_-$, due to the sources in the second medium. The difference of the two expressions is the net energy transfer due to the temperature difference of the two bodies.

It is clear that whatever functions $\epsilon_1(\omega)$, $\epsilon_2(\omega)$ one takes, the net energy transfer expression must be zero if the temperatures T_1 and T_2 occurring in the Bose-Einstein factor of the two media are equal. Thus the differential energy transfer

$$W = \lim_{(T_1 - T_2) \to 0} \left| \frac{S_z(d_+) - S_z(0_-)}{T_1 - T_2} \right|$$

originates entirely from the temperature derivative of the Bose-Einstein factor and there is no contribution from the temperature dependence of ϵ_1 and ϵ_2. The values for $\epsilon_1(\omega)$ and $\epsilon_2(\omega)$ to be used are those pertaining to the working temperature $T_1 = T_2$. In the further discussion we specialize to the case of identical media, i. e., $\epsilon \equiv \epsilon_1 = \epsilon_2$.

It is of importance to note that, in this calculation, multiple reflection at the two boundaries is fully taken into account. The corresponding interference effects constitute one reason for a dependence of the energy transfer on the distance d. The second reason is that, in contradistinction to the first example, vacuum waves with imaginary k_{zv} values now contribute to the net energy flow, and especially at small-d values this will be an important contribution.

For the calculation of the Poynting vector $\vec{S}$ at $z = d_+$ we need the tensors

$$\vec{e}, \vec{h}(k_x, 0, d_+, z', \omega) \qquad (z' < 0).$$

These tensors are determined by solving the Maxwell problem, that, for each polarization state, involves six waves and six boundary conditions at the boundaries of the media and at the source plane. For the calculation of S_z we need the result for the following components:

$$h_{xy} = -ck_z\omega^{-1}e_{yy} = 8\pi k_{zv}k_z c^{-1}C_{\perp}^{-1} e^{ik_z' z'} \;,$$

$$h_{yx} = -k_z k_x^{-1} h_{yz} = \epsilon\omega c^{-1}k_z^{-1} e_{xx} = -\epsilon\omega c^{-1}k_x^{-1} e_{xz}$$

$$= -8\pi k_{zv}k_z\epsilon c^{-1}C_{\parallel}^{-1} e^{ik_z' z'} \;,$$

$$e_{xy} = e_{yx} = e_{yz} = h_{xx} = h_{xz} = h_{yy} = 0 \;,$$

where

$$C_{\parallel} = (\epsilon k_{zv} + k_z)^2 e^{ik_{zv}d} - (\epsilon k_{zv} - k_z)^2 e^{-ik_{zv}d} \;,$$

$$C_{\perp} = (k_{zv} + k_z)^2 e^{ik_{zv}d} - (k_{zv} - k_z)^2 e^{-ik_{zv}d} \;.$$

Because of azimuthal symmetry, in Eq. (9) we can substitute for $\vec{e}$ and $\vec{h}$ the quantities at $k_y = 0$ which we have just calculated and replace $dk_x dk_y$ by $2\pi k_x dk_x$, integrating between 0 and ∞. We finally obtain

$$S_z(d_+) = \int_0^{\infty} d\omega \int_0^{\infty} dk_x \, 16(2\pi)^{-2} k_x |k_{zv}|^2$$

$$\times \hbar\omega(e^{\hbar\omega/kT_1} - 1)^{-1}$$

$$\times \{[\text{Re}(\epsilon k_z^*)]^2 |C_{\parallel}|^{-2} + (\text{Re}k_z)^2 |C_{\perp}|^{-2}\} \;. \quad (19)$$

The differential energy transfer is

$$W = \frac{\partial S_z(d_+)}{\partial T_1} \;, \qquad (20)$$

the differentiation being understood to be with respect to the explicit T dependence in the Bose-Einstein factor only.

VI. STRUCTURE OF THE RESULT

The result as given by Eqs. (19) and (20) exhibits in the curly brackets the additive contributions of the two independent polarizations. These contributions have quite similar structures and may thus be treated together throughout this section.

The distinction between real and imaginary k_{zv} is quite interesting, though not of great physical importance in the present problem. It is the distinction between waves propagating undamped across the vacuum gap and the evanescent waves reaching over the gap. The contributions corresponding to these two types of waves we shall denote as W^{sin} and W^{exp}, respectively: W^{sin} involves the k_x-integration interval $[0, \omega/c]$; restriction to the interval $[\omega/c, \infty]$ yields W^{exp}. Then, we have

$$W = W^{\text{sin}} + W^{\text{exp}} \;; \qquad (21)$$

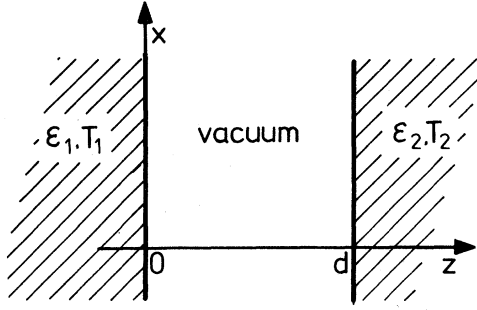both contributions will now be separately discussed.

FIG. 1. Geometric situation for the calculation of the radiative heat transfer between bodies a distance d apart.

In $W^{\sin}$ it is rewarding to introduce the reflectivities $R_{||}$ and $R_{\perp}$ already used [cf. Eq. (18)]. One then obtains

$$W^{\sin} = \int_0^{\infty} d\omega \int_0^{\omega/c} dk_x (2\pi)^{-2} k_x (t_{||}^{\sin} + t_{\perp}^{\sin})$$

$$\times \frac{\partial [\hbar\omega/(e^{\hbar\omega/kT} - 1)]}{\partial T} \quad , \quad (22)$$

where

$$t_{||}^{\sin} = \frac{(1 - R_{||})^2}{|1 - R_{||} e^{i(\beta_{||} - 2k_{zv}d)}|^2} \qquad t_{\perp}^{\sin} = \frac{(1 - R_{\perp})^2}{|1 - R_{\perp} e^{i(\beta_{\perp} - 2k_{zv}d)}|^2}$$

$$\quad (23)$$

and

$$\beta_{||} = 2 \arg[(\epsilon k_{zv} - k_z)(\epsilon k_{zv} + k_z)^*] \quad ,$$

$$\beta_{\perp} = 2 \arg[(k_{zv} - k_z)(k_{zv} + k_z)^*] \quad .$$

The quantities $t_{||}^{\sin}$ and $t_{\perp}^{\sin}$ can be considered as the energy transmission coefficients for a wave with real $k_x \leqslant \omega/c$, passing the surface at $z = 0_-$ and being detected at $z = d_+$. This can easily be verified by tracing the multiple reflections of such a light ray through the optical system and summing the amplitudes of the transmitted waves, taking $\frac{1}{2}\beta_{||}$ and $\frac{1}{2}\beta_{\perp}$ as the phase jumps at reflection so as to account properly for interference effects. It is clear that in the present simple geometry Eq. (22) could have been obtained directly from Kirchhoff's law by substituting for $1 - R$ the transmission coefficients $t^{\sin}$ pertaining to the new geometry. In order to illustrate the structure of the transmission coefficients we shall consider the case of a metal. In Fig. 2, $t_{||}^{\sin}$ and $t_{\perp}^{\sin}$ are set out against k_x and d at fixed vacuum wavelength $\lambda = 5$ μm for a dielectric constant representative of metals; we now only consider $0 \leqslant k_x \leqslant \omega/c$.

As a function of d the transmission coefficients have rigorous periodicity, the period being πk_{zv}^{-1} and growing continuously from $\frac{1}{2}\lambda$ to ∞ when k_x grows from 0 to ω/c. In the figure the observed sharpness of the ribs results from high reflectiv-

ities $R_{||}$ and $R_{\perp}$, which in turn are a consequence of the high absolute value of ϵ encountered in metals. The reflectivities pertaining to the case of Fig. 2 are shown in Fig. 3.

In $W^{\exp}$ the integrand can be rewritten as follows. Since now $k_x \geqslant \omega/c$, we define

$$k_{zv} = -i\kappa \quad \text{with} \quad \kappa = (k_x^2 - \omega^2/c^2)^{1/2} \geqslant 0 \quad ,$$

yielding

$$W^{\exp} = \int_0^{\infty} d\omega \int_{\omega/c}^{\infty} dk_x (2\pi)^{-2} k_x (t_{||}^{\exp} + t_{\perp}^{\exp})$$

$$\times \frac{\partial [\hbar\omega/(e^{\hbar\omega/kT} - 1)]}{\partial T} \quad , \quad (24)$$

with

$$t_{||}^{\exp} = \frac{1 - \cos\chi_{||}}{\cosh[2\kappa(d - \delta_{||})] - \cos\chi_{||}} \quad ,$$

$$\quad (25)$$

$$t_{\perp}^{\exp} = \frac{1 - \cos\chi_{\perp}}{\cosh[2\kappa(d - \delta_{\perp})] - \cos\chi_{\perp}} \quad ,$$

and

$$e^{\kappa\delta_{||}} = \left| \frac{i\kappa\epsilon + k_z}{i\kappa\epsilon - k_z} \right|^2 \quad , \quad e^{\kappa\delta_{\perp}} = \left| \frac{i\kappa + k_z}{i\kappa - k_z} \right|^2 \quad ,$$

$$\chi_{||} = 2 \arg[(-i\kappa\epsilon + k_z)(-i\kappa\epsilon - k_z)^*] \quad ,$$

$$\chi_{\perp} = 2 \arg[(-i\kappa + k_z)(-i\kappa - k_z)^*] \quad .$$

Again $t_{||}^{\exp}$ and $t_{\perp}^{\exp}$ can be considered as energy transmission coefficients for waves with real k_x, where now $k_x > \omega/c$. However, Eq. (24) could not have been obtained directly from the Kirchhoff expression, simply because Kirchhoff's law only applies to waves with $k_x < \omega/c$ and there is no immediate thermodynamic argument leading to a corresponding expression for $k_x > \omega/c$ (i.e., complex angles of propagation in vacuum).

Specializing to the case of a metal, one can show that, as a result of $\text{Re}\,\epsilon < 0$ and $\text{Im}\,\epsilon < 0$ (as is the case in most metals for wavelengths above 1 μm)

$$\delta_{||} > 0 \quad \text{and} \quad \delta_{\perp} < 0 \quad .$$

The d dependence of $t_{||}^{\exp}$ and $t_{\perp}^{\exp}$ is easy to visualize and is also illustrated in Fig. 2 as the continuation of $t_{||}^{\sin}$ and $t_{\perp}^{\sin}$ for $k_x \geqslant \omega/c$. When $d \to \infty$, the transmission now falls off as $e^{-2\kappa d}$, as one would expect.

A remarkable fact is that for a wave of parallel polarization which suffers total reflection in the presence of only vacuum at $z > 0$ (i.e., $k_x > \omega/c$), there is a certain value of d, namely, $\delta_{||}$, such that we have total transmission of that wave to an opposite identical body.
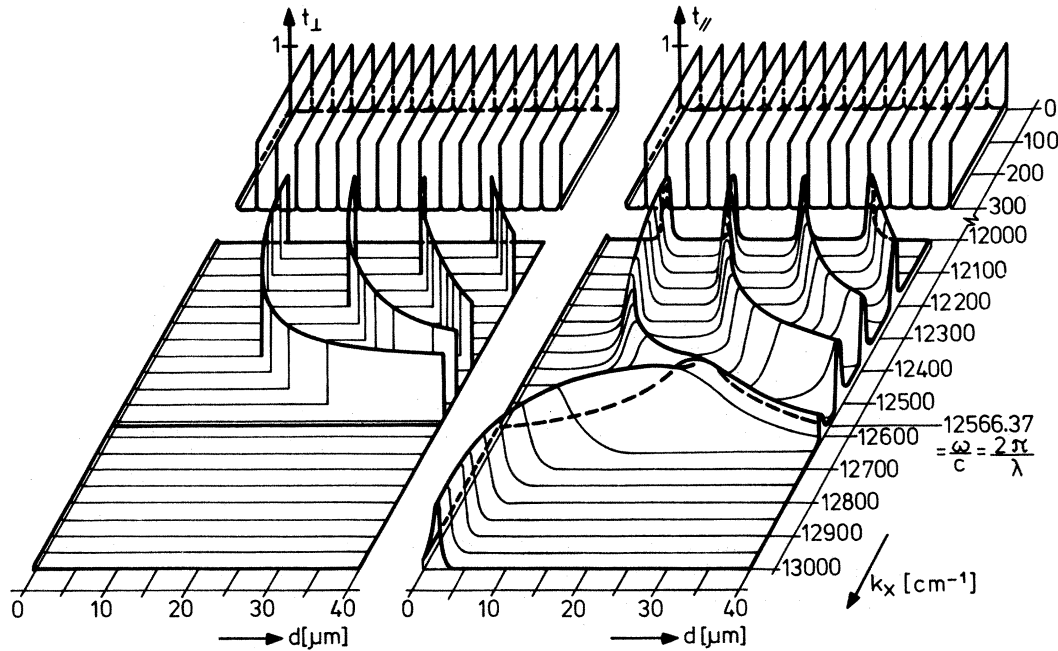
FIG. 2. Energy transmission coefficients $t_\perp$, $t_\parallel$ for waves of vacuum wavelength $\lambda = 5\,\mu m$ as functions of gap width d and wave vector component $k_x > 0$ along the surfaces of the gap, with the dielectric constant $\epsilon = -200 - i130$. "Traveling" waves have $0 \leq k_x \leq \omega/c$; "evanescent" waves have $k_x \geq \omega/c$.

Let us now consider what conclusions can be drawn as to the behavior of W in view of the structure of the integrand as depicted in Fig. 2. First of all for $d \to \infty$, integration over k_x means an integration over an infinitely densely ribbed structure. With the aid of the averaging procedure

$$\left\langle \lim_{d \to \infty} t_\parallel^{\sin} \right\rangle = \frac{1}{2\pi} \int_0^{2\pi} d\psi \, \frac{(1 - R_\parallel)^2}{|1 - R_\parallel e^{i\psi}|^2} = \frac{1 - R_\parallel}{1 + R_\parallel} \quad ,$$

$$(26)$$

$$\left\langle \lim_{d \to \infty} t_\perp^{\sin} \right\rangle = \frac{1 - R_\perp}{1 + R_\perp}$$

(where $R_\parallel$ and $R_\perp$ still depend on k_x and ω) we find, since $W^{\exp} \to 0$ as $d \to \infty$, the exact expression

$$W(d \to \infty) = \int_0^\infty d\omega \int_0^{\omega/c} dk_x (2\pi)^{-2} k_x$$

$$\times \left[(1 - R_\parallel)/(1 + R_\parallel) + (1 - R_\perp)/(1 + R_\perp) \right]$$

$$\times \frac{\partial [\hbar\omega/(e^{\hbar\omega/kT} - 1)]}{\partial T} \quad , \quad (27)$$

independent of d. This result is not surprising; it could have been obtained by tracing a ray of light through the optical system, adding transmitted intensities rather than transmitted amplitudes.

For smaller values of d, i.e., d gradually decreasing to the order of c/ω at the frequency considered, Fig. 2 shows how fewer and fewer peaks contribute to the integration over k_x. Of course,
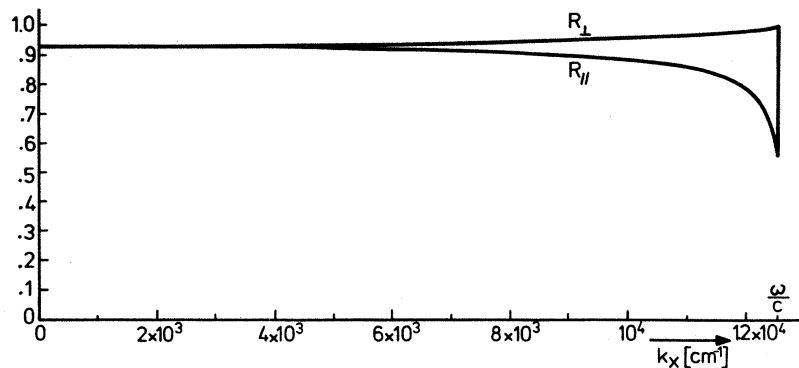

FIG. 3. Energy reflection coefficients $R_\parallel(k_x)$ and $R_\perp(k_x)$ between vacuum and a medium of dielectric constant $\epsilon = -200 - i130$, for waves of vacuum wavelength $\lambda = 5\,\mu m$.
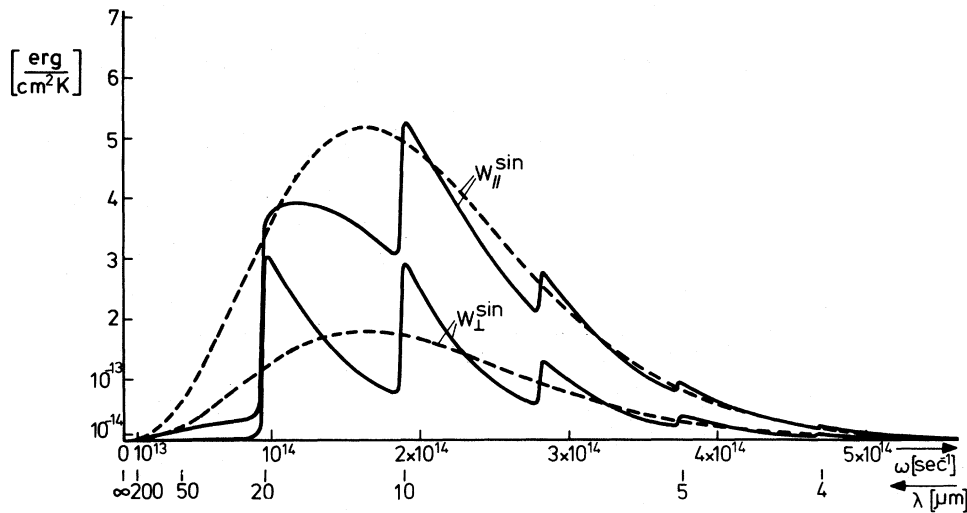
FIG. 4. Frequency spectrum of the contributions $W_{\parallel}^{\sin}$ and $W_{\perp}^{\sin}$ to the net heat transfer at the temperature $T = 315\,\mathrm{K}$ for $d = 10\,\mu m$ (solid curves) and $d \to \infty$ (dashed curves) obtained by numerical calculation, using the dielectric constant represented by the curves 4 and 5 in Fig. 8. The corresponding scale of vacuum wavelengths is included.

the number of these peaks depends on the particular frequency. Indeed, the frequency spectrum of $W^{\sin}$ at a given value of d (cf. Fig. 4) shows a number of steep rises at those frequencies where a new peak enters the integration interval over k_x at $k_x = 0$, i.e., at the frequencies $\omega \approx n(c/d)$ $(n = 1, 2, \dots)$. In Fig. 4 the frequency spectrum of $W^{\sin}$ is shown for the two polarization states, while for comparison the frequency distribution at

$d \to \infty$ is also shown. Data used are given in the caption.

For a given frequency (for which we may take the dominant frequency in the Planck radiation expression) and with $d \approx c/\omega$ we no longer find peaks in the integration range $0 \leqslant k_x \leqslant \omega/c$. This will have a strong diminishing effect on the value of $W^{\sin}$. On the other hand $W^{\exp}$ is now already increasing strongly with decreasing d,
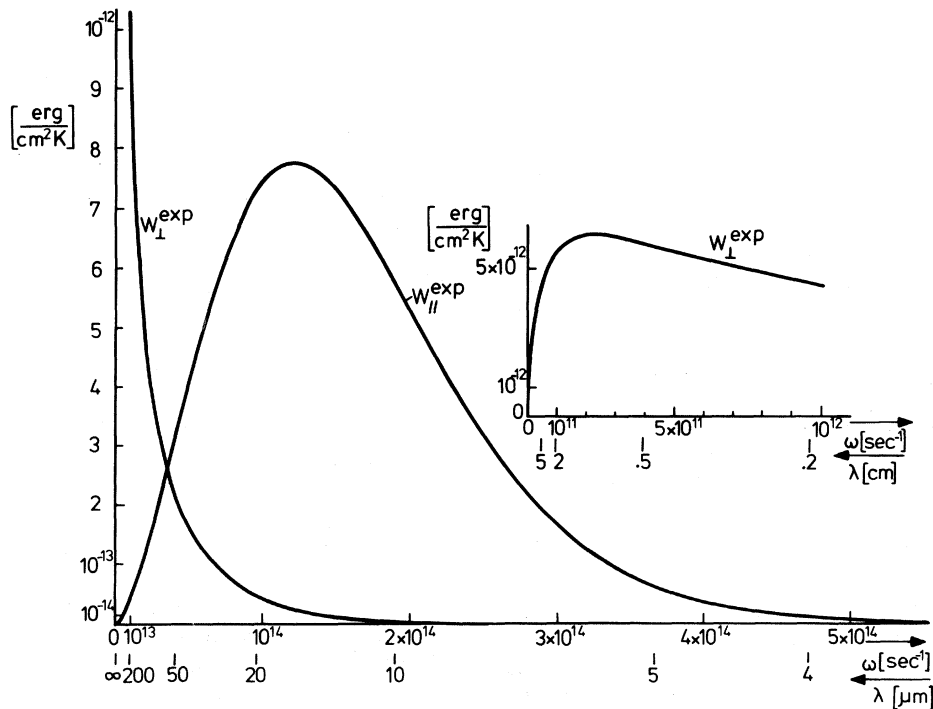

FIG. 5. Frequency spectrum of the contributions $W_{\parallel}^{\exp}$ and $W_{\perp}^{\exp}$ to the net heat transfer for $d = 2\,\mu m$, further data as in Fig. 4. The inset shows the low-frequency behavior of $W_{\perp}^{\exp}$ (note the unit of λ).

at first mainly because of the peak in the $\parallel$ polarization at $k_x > \omega/c$. The importance of W^{exp} is illustrated by Fig. 5, which gives the frequency spectrum of the $\parallel$ polarization contained in W^{exp} for a typical distance of this order; note that this spectrum is already comparable in magnitude to the spectrum of W^{sin} at the much larger distance in Fig. 4. Also shown in Fig. 5 is the frequency spectrum for the $\perp$ polarization contained in W^{exp}: The center of gravity of this distribution is very much at the low-frequency side. In terms of the behavior of t^{exp} as depicted in Fig. 2, it originates from the rise near $d = 0$, which is tremendously more pronounced at low frequencies. While with decreasing d the $\parallel$ polarization part of W^{exp} rises above the W^{sin} contribution, it in turn is rapidly overtaken by the $\perp$ polarization part of W^{exp}.

In Sec. VII we shall try and give a somewhat more precise discussion of the qualitative points just mentioned, including the d, T, and ϵ dependence to be expected in a model conductor with purely imaginary ϵ (proportional to ω^{-1}).

VII. APPROXIMATE INTEGRATION

Consider W^{sin} first. Its $d \to \infty$ limit can be obtained with some accuracy under the assumption $|\epsilon| \gg 1$. If we write $\epsilon = -i4\pi\sigma/\omega$ for a substance of conductivity σ, this assumption is equivalent to

$$T/\sigma \ll 2 \times 10^{-11} \tag{28}$$

(in Gaussian units), where Wien's relation

$$T\lambda_{max} = 0.2hc/k \tag{29}$$

between temperature and dominant vacuum wavelength has been used.

Now we obtain, using $\int_0^\infty dx\, x^{9/2} e^x/(e^x-1)^2 = 55.2$ for the frequency integration, from Eq. (27),

$$W^{sin}(d \to \infty) \approx \frac{4}{3} \frac{55.2}{(2\pi)^{5/2}} \frac{k^{9/2}}{\hbar^{7/2}c^2} \frac{T^{7/2}}{\sigma^{1/2}}$$

$$= 93.5 \frac{T^{7/2}}{\sigma^{1/2}} , \tag{30}$$

exhibiting clearly temperature and conductivity dependence (σ may still depend on temperature, e.g., $\sigma \propto T^{-1}$).

Equation (30) may be easily understood in terms of the Stefan-Boltzmann law, which predicts a differential heat transfer proportional to $dT^4/dT \propto T^3$ and proportional to the averaged transmission coefficient ($\propto T^{1/2}\sigma^{-1/2}$).

A crude idea of the decrease of W^{sin} for small-d values can be obtained by cutting off the frequency integration leading to Eq. (30) below the first rise in the spectrum (cf. Fig. 4), i.e., below $\omega \approx \pi c/d$. The distance d^* of largest $\partial w^{sin}/\partial d$ then satisfies $d^* \approx 0.163 T^{-1}$ or $d^* \approx 0.57\lambda_{max}$. This approximation by frequency cutoff is very un-

satisfactory in the $d \to 0$ limit. This is of no consequence as W^{exp} has much larger values then.

As regards the contribution W^{exp}, it is convenient to use the following exact expression, obtained from Eq. (24):

$$W^{exp} = \int_0^\infty d\omega (2\pi)^{-2}[I_\parallel + I_\perp] \frac{\partial[\hbar\omega/(e^{\hbar\omega/kT} - 1)]}{\partial T} , \tag{31}$$

with

$$I_\parallel = \int_0^\infty d\kappa\, \kappa \frac{[\text{Re}(\epsilon k_z^*)]^2/|\epsilon k_z|^2}{|\cosh\kappa d + \frac{1}{2}i[k_z/(\epsilon\kappa) - \epsilon\kappa/k_z]\sinh\kappa d|^2} , \tag{32}$$

$$I_\perp = \int_0^\infty d\kappa\, \kappa \frac{(\text{Re}\,k_z)^2/|k_z|^2}{|\cosh\kappa d + \frac{1}{2}i(k_z/\kappa - \kappa/k_z)\sinh\kappa d|^2} , \tag{33}$$

where $k_x dk_x = -k_{zv} dk_{zv} = \kappa d\kappa$ has been used.

To treat these integrals we again assume that $|\epsilon| \gg 1$ holds for all relevant frequencies. We define $\rho_\parallel = \arg(k_z/\epsilon)$ and $\rho_\perp = \arg k_z$.

For $d \lesssim |\epsilon|^{1/2}\lambda/(2\pi)$ we then obtain

$$I_\parallel \approx \frac{\omega\cos\rho_\parallel}{|\epsilon|^{1/2}cd} \int_{-\tan\rho_\parallel}^\infty dx \frac{1}{1+x^2}$$

$$= (\tfrac{1}{2}\pi + \rho_\parallel)\frac{\omega}{|\epsilon|^{1/2}cd} . \tag{34}$$

For $d \gg |\epsilon|^{1/2}\lambda/(2\pi)$ one obtains, using $\int_0^\infty dx\, x^3/\sinh^2 x = 1.803$,

$$I_\parallel \approx 7.212\cos^2\rho_\parallel c^2\omega^{-2}|\epsilon|\, d^{-4} . \tag{35}$$

The point $d \approx |\epsilon|^{1/2}\lambda/(2\pi)$ separating Eq. (34) from Eq. (35) corresponds to the maximum value of $\delta_\parallel$ in Eq. (25).

For $d \ll |\epsilon|^{-1/2}\lambda/(2\pi)$, $I_\perp$ becomes independent of d:

$$I_\perp \approx \tfrac{1}{2}\cos^2\rho_\perp|\epsilon|\omega^2 c^{-2} . \tag{36}$$

For $d \gg |\epsilon|^{-1/2}\lambda/(2\pi)$, we have

$$I_\perp \approx 7.212\cos^2\rho_\perp c^2\omega^{-2}|\epsilon|^{-1}d^{-4} . \tag{37}$$

The Bose-Einstein factor of Eq. (31) is constant for low frequencies. Thus, the low-frequency end of the spectrum will be largely shaped by $I_\parallel$ and $I_\perp$ (cf. Figs. 4 and 5). Taking for example $d \approx \lambda$, so that Eqs. (34) and (37) apply, we see that $I_\parallel$ falls rapidly to zero as $\omega \to 0$, because $I_\parallel \propto \omega|\epsilon|^{-1/2}$. However,

$$I_\perp \propto \cos^2\rho_\perp \omega^{-2}|\epsilon|^{-1} \propto \cos^2\rho_\perp \omega^{-1} ,$$

so that $I_\perp$ only falls to zero when $\cos^2\rho_\perp$ compensates the diverging factor ω^{-1}; it is possible to show that this compensation happens near a frequency ω_{min} roughly determined by the relation $|\epsilon(\omega_{min})|\omega_{min}^2 \approx c^2 d^{-2}$, which becomes, for $|\epsilon| = 4\pi\sigma/\omega$,
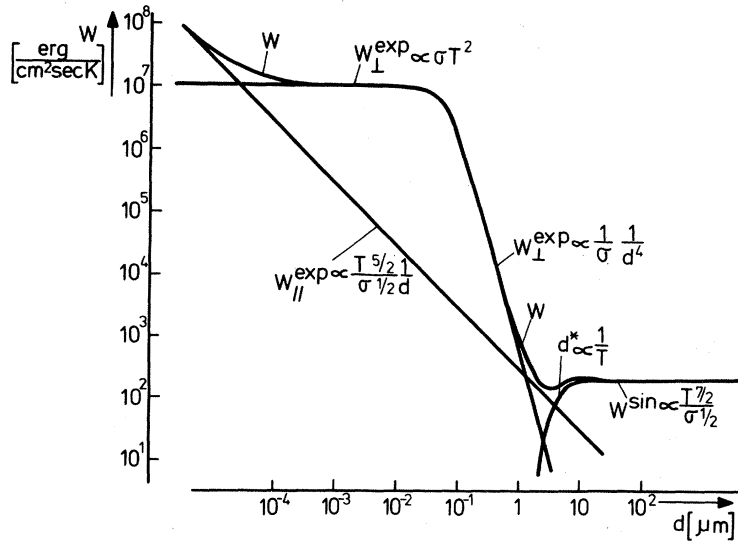
FIG. 6. Approximate integrated contributions to the net heat transfer as obtained in Sec. VII and their sum W as functions of d in the case $T = 315$ K, $\epsilon = -i4\pi\sigma\omega^{-1}$, and $\sigma = 7.0 \times 10^{16}$ sec^{-1}. $W^{\sin}$ has been calculated with the frequency cutoff described in the text. The T, σ, and d dependence of the various contributions and of d^* are included. Below $d = 10^{-2}\,\mu$m $= 100$ Å these curves lose their physical meaningfulness, owing to electronic and atomic effects.

$$\omega_{\min} \approx (4\pi)^{-1} c^2 \sigma^{-1} d^{-2} \quad . \tag{38}$$

To integrate these results over frequency we specify that $\epsilon = -i4\pi\sigma/\omega$. The various regions of validity of the expressions obtained will be described by comparing d to the dominant wavelength $\lambda_{\max}$ defined by Eq. (29).

For $d \ll |\epsilon(\lambda_{\max})|^{1/2}\lambda_{\max}/(2\pi)$, since

$$\int_0^\infty dx\, x^{7/2} e^x/(e^x - 1)^2 = 13.1 \quad ,$$

Eqs. (31) and (34) yield

$$W_\parallel^{\exp} \approx 0.156\, k^{7/2} c^{-1} \hbar^{-5/2}\, T^{5/2} \sigma^{-1/2} d^{-1}$$

$$\approx 4.46\ T^{5/2} \sigma^{-1/2} d^{-1} \quad . \tag{39}$$

Equation (35) gives a heat transfer negligible with

respect to $W^{\sin}$.

For

$$d \ll |\epsilon(\lambda_{\max})|^{-1/2}\lambda_{\max}/(2\pi) \quad ,$$

the $\perp$ polarization yields, with $\int_0^\infty dx\, x^3 e^x/(e^x - 1)^2 = 7.20$,

$$W_\perp^{\exp} \approx 0.574\, k^3 \hbar^{-2} c^{-2} \sigma T^2 = 1.52 \times 10^{-15} \sigma T^2 \quad . \tag{40}$$

For

$$d \gg |\epsilon(\lambda_{\max})|^{-1/2}\lambda_{\max}/(2\pi)$$

we have, using Eq. (37),

$$W_\perp^{\exp} \approx 7.3 \times 10^{-3} kc^2 \sigma^{-1} d^{-4}$$

$$\times [5.6 + \ln(4\pi\, 10^{-2} k\hbar^{-1} c^{-2}) + \ln(\sigma T d^2)]$$

$$= 908\sigma^{-1} d^{-4}[\ln(\sigma T d^2) - 20.4] \quad , \tag{41}$$
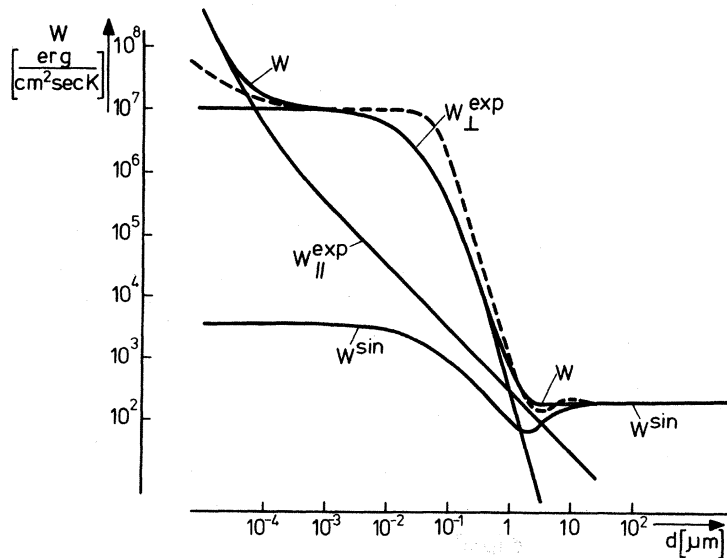

FIG. 7. Numerically integrated contributions to the net heat transfer and their sum W as functions of d for the case of Fig. 6, with (dashed curve) the total approximate result of Fig. 6 superimposed.
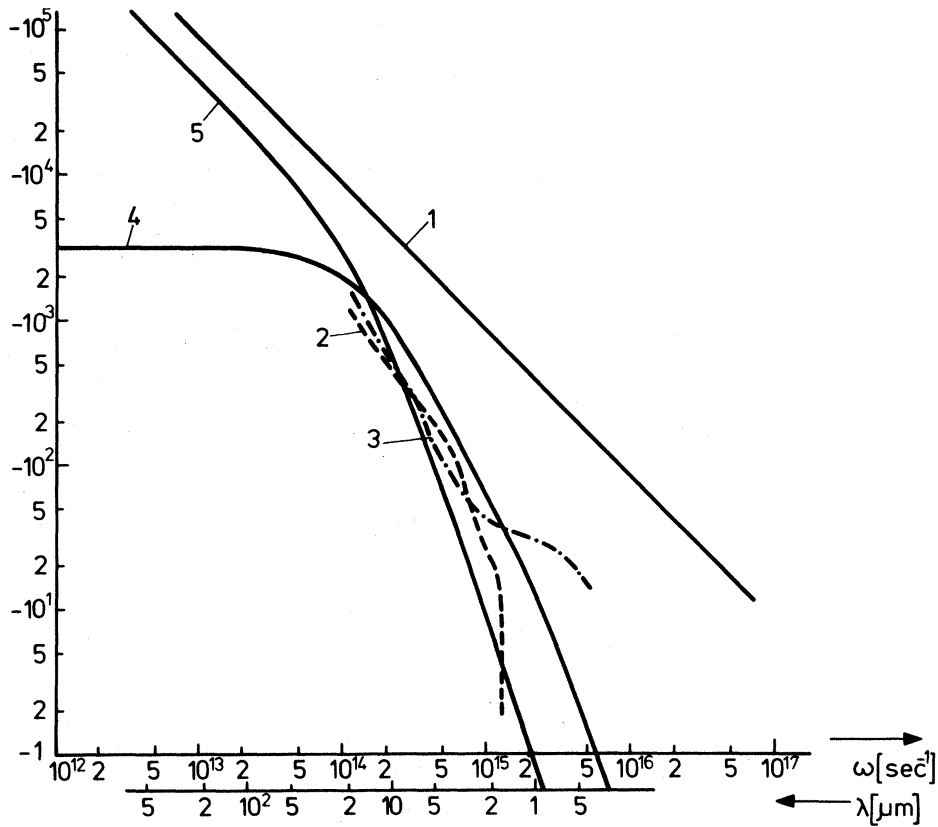
FIG. 8. Dielectric constants as functions of frequency ω (and vacuum wavelength λ): curve 1: $\text{Im}\epsilon = -4\pi\sigma\omega^{-1}$ with $\sigma = 7.0 \times 10^{16}\,\text{sec}^{-1}$; this choice of $\epsilon(\omega)$ (with $\text{Re}\epsilon = 0$) is used in the approximate integrations of Sec. VII, as represented in Figs. 6 and 7; curves 2 and 3: $\text{Re}\,\epsilon$ and $\text{Im}\epsilon$, respectively, as measured by Lenham and Treherne; curves 4 and 5: $\text{Re}\,\epsilon$ $= 1 - 4\pi\sigma\omega_0(\omega^2 + \omega_0^2)^{-1}$ and $\text{Im}\epsilon = -4\pi\sigma\omega_0^2\omega^{-1}(\omega^2 + \omega_0^2)^{-1}$, respectively, with $\sigma = 3.5 \times 10^{16}\,\text{sec}^{-1}$, $\omega_0 = 1.41 \times 10^{14}\,\text{sec}^{-1}$, as an approximation to the measured values (curves 2 and 3); this choice of ϵ is used in the computation of Fig. 9.
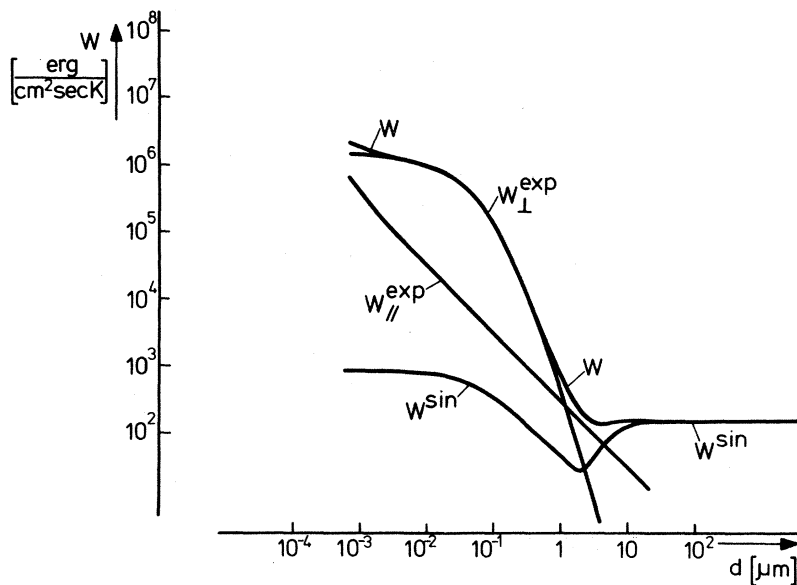
FIG. 9. Contributions to the net heat transfer and their sum W as functions of d as calculated at $T = 315$ K with the dielectric constant represented by the curves 4 and 5 in Fig. 8.

because

$$\int_{x_{\min}}^{\infty} dx\, x e^x /(e^x - 1)^2$$

$$\approx \int_{x_{\min}}^{0.01} dx/x + \int_{0.01}^{\infty} dx\, x e^x /(e^x - 1)^2$$

$$\approx \ln(0.01\, x_{\min}^{-1}) + 5.6 \quad, \tag{42}$$

where $x_{\min} = \hbar \omega_{\min}/kT$ [cf. Eq. (38)].

The theoretical approximate results as functions of d are represented in a specific case in Fig. 6; here $\sigma = 7.0 \times 10^{16}$ sec^{-1} and $T = 315$ K, so that $\lambda_{\max} \approx 9.2$ μm. Notice the remarkably large contribution of $W^{\bullet\,xp}$ owing to a very intense spectrum.

With the knowledge of the d, σ, and T dependence of the total heat transfer as given by the above approximations (and brought together in Fig. 6) we can, for example, predict that the dip occurring near $d = \frac{1}{3}\lambda_{\max}$ will disappear if σ is chosen smaller; then also the height of the shoulder diminishes and sensibly approaches the $d \to \infty$ value; and vice versa, large conductivities favor a dip and a large ratio of shoulder height to $d \to \infty$ value.

A temperature increase will in first approximation shift the dip up along the d^{-4} slope in Fig. 6, while it reduces the ratio of shoulder height to $d \to \infty$ value.

One should in fact take into account the temperature dependence of σ (e.g., $\sigma \propto T^{-1}$), but this only influences quantitatively the features just mentioned.

Fig. 7 shows computed result based on the exact formulas in the same physical situation. These confirm the discussed expectations.

In the foregoing example, condition (28) was satisfied. We now consider a more realistic situation and try to treat the case of chromium near room temperature. In the (infrared) frequency region corresponding to such temperatures, the condition $|\epsilon| \gg 1$ is not everywhere fulfilled for chromium. Thus, the analytic approximations lose their reliability and we have to concentrate on numerical integration.

To obtain $\epsilon(\omega)$ for chromium we apply the method of curve fitting of a theoretical expression for

$\epsilon(\omega)$ satisfying the Kramers-Kronig relations to experimental optical data (taken over from Ref. 6 and later measurements by these authors). The expression Im$\epsilon = -4\pi\sigma\omega^{-1}$ has the free parameter σ and gives Reϵ through the Kramers-Kronig relations. But it is simpler and more realistic to use an expression provided by Drude's theory of conductivity, incorporating a low-frequency conductivity σ and a mean free flight time ω_0^{-1}, which we may consider as free parameters:

$$\text{Re}\epsilon = 1 - \frac{4\pi\sigma\omega_0}{\omega^2 + \omega_0^2} \quad, \quad \text{Im}\epsilon = -\frac{4\pi\sigma\omega_0^2}{\omega(\omega^2 + \omega_0^2)} \quad. \tag{43}$$

A reasonable fit to experimental data in the frequency range of interest is found for $\sigma = 3.5 \times 10^{16}$ sec^{-1} and $\omega_0 = 1.41 \times 10^{14}$ sec^{-1}. The resulting $\epsilon(\omega)$ is represented in Fig. 8, together with experimental curves and Im$\epsilon = -4\pi\sigma\omega^{-1}$ as used in the preceding example. And Fig. 9 shows the corresponding heat transfer W.

Comparison of Figs. 9 and 7 shows at once that the $d \to \infty$ value has diminished rather than been augmented, although $|\epsilon|$ has diminished: The reason for this lies in the fact that now the argument of ϵ has changed markedly in the short-wavelength region. Nevertheless, the curve of Fig. 9 has the same general characteristic shape as that of Fig. 7; in particular, the distance at which the small-separation effects appear has not changed, being in first approximation only dependent on temperature.

In Ref. 5, Hargreaves published measurements of radiative heat transfer between flat chromium bodies with a mean temperature of $T \approx 315$ K in the separation range $1 < d < 10$ μm. We find very good agreement with experiment as regards the shape of the curves and the critical distance below which the small-separation effect becomes noticeable.

The absolute values of the heat currents, though of the same order of magnitude, do not coincide, however, not even for $d \to \infty$: It appears after examination of more recent, as yet unpublished, measurements by the same author that the discrepancy lies in a difference between bulk chromium (on which our calculations are based) and the chromium layers used in the experiments.

[1]S. M. Rytov, *Theory of Electric Fluctuations and Thermal Radiation* (Air Force Cambridge Research Center, Bedford, Mass., 1959), AFCRC-TR-59-162.

[2]M. A. Leontovich and S. M. Rytov, Zh. Eksperim. i Teor. Fiz. **23**, 246 (1952).

[3]E. G. Cravalho, C. L. Tien, and R. P. Caren, Trans. ASME Ser. C **89**, 351 (1967).

[4]A. Olivei, Rev. Phys. Appl. **3**, 225 (1968).

[5]C. M. Hargreaves, Phys. Letters **30A**, 491 (1969).

[6]A. P. Lenham and D. M. Treherne, in *Optical Properties and Electronic Structure of Metals and Alloys*, edited by F. Abelés (North-Holland, Amsterdam, 1966), p. 196; and J. Opt. Soc. Am. **56**, 1137 (1966).